Liquid Crystals
Publication details, including instructions for authors and subscription information:
http://www.informaworld.com/smpp/title~content=t713926090

Symmetric and non-symmetric chiral liquid crystal dimers

T. Donaldson[a]; H. Staesche[a]; Z. B. Lu[a]; P. A. Henderson[a]; M. F. Achard[b]; C. T. Imrie[a]
[a] Chemistry, School of Natural and Computing Sciences, University of Aberdeen, Aberdeen, UK [b] Centre de Recherche Paul Pascal, Université Bordeaux I, Pessac, France

Online publication date: 16 August 2010

To cite this Article Donaldson, T. , Staesche, H. , Lu, Z. B. , Henderson, P. A. , Achard, M. F. and Imrie, C. T.(2010) 'Symmetric and non-symmetric chiral liquid crystal dimers', Liquid Crystals, 37: 8, 1097 — 1110
To link to this Article: DOI: 10.1080/02678292.2010.494412
URL: http://dx.doi.org/10.1080/02678292.2010.494412

Liquid Crystals,
Vol. 37, No. 8, August 2010, 1097–1110

Taylor & Francis
Taylor & Francis Group

Symmetric and non-symmetric chiral liquid crystal dimers

T. Donaldson[a], H. Staesche[a], Z.B. Lu[a], P.A. Henderson[a], M.F. Achard[b] and C.T. Imrie[a]*

[a]*Chemistry, School of Natural and Computing Sciences, University of Aberdeen, Aberdeen, UK;* [b]*Centre de Recherche Paul Pascal, Université Bordeaux I, Pessac, France*

(*Received 25 February 2010; final version received 13 May 2010*)

The synthesis and characterisation of three sets of non-symmetric liquid crystal dimers consisting of a cholesteryl-based unit and either 4-methoxybiphenyl, 4-cyanobiphenyl or (*S*)-2-methylbutyl 4′oxybiphenyl-4-carboxylate are described. The transitional properties of these non-symmetric dimers are compared to those of the corresponding parent symmetric dimers. The symmetric dimers exhibit only chiral nematic or nematic phase behaviour. By contrast, members of the non-symmetric dimer series containing either 4-cyanobiphenyl or (*S*)-2-methylbutyl 4′-oxybiphenyl-4-carboxylate groups exhibit smectic behaviour. The former series show an interdigitated smectic A phase while for the latter the structure of the smectic A phase depends on the length of the flexible spacer. Specifically, for short spacer lengths a monolayer arrangement is seen while for long spacers an intercalated smectic A phase is formed. For an intermediate spacer length, the small-angle X-ray scattering pattern for the intercalated smectic A phase reveals short-range incommensurate structural fluctuations associated with the monolayer smectic A phase. The driving force for the formation of the intercalated phase may be an electrostatic interaction between the electron rich carbonyl linking group attached to the cholesteryl unit and the electron deficient aromatic unit while the monolayer arrangement may be stabilised by the van der Waals interactions between the cholesteryl unit and the alkyl chains. Blue phases are observed only for a small number of these non-symmetric dimers and these all contain an odd-membered spacer. This is in accord with the rather general observation that blue phases are observed for odd-membered non-symmetric dimers and not their even-membered counterparts.

Keywords: liquid crystal dimers; cholestryl-based mesogen; intercalated smectic A phases

1. Introduction

Over the last two decades there has been a dramatic increase in the diversity of molecular architectures containing rod-like mesogenic units known to exhibit liquid crystal behaviour [1]. Of these new structures, liquid crystal oligomers have attracted much research interest and consist of molecules composed of semi-rigid mesogenic units linked via flexible spacers [2–5]. The simplest of these oligomers are liquid crystal dimers which consist of molecules containing just two mesogenic units connected via a flexible spacer [2–4]. This class of materials exhibits fascinating phase behaviour, quite different to that observed for conventional low molar mass liquid crystals composed of molecules consisting of a single semi-rigid or mesogenic core attached to which are one or two terminal alkyl chains. Some recent reports of liquid crystal dimers include: hydrogen-bonded dimers [6–8]; phase behaviour in carbonate-linked [9] and bent odd-membered dimers [10]; dimers containing anthracene-based groups [11]; the flexoelectric properties of dimers [12, 13] and light emitting dimers [14]. Liquid crystal dimers may be divided into two broad classes: symmetric and non-symmetric. In a symmetric liquid crystal dimer the two mesogenic units are identical whereas they are different in a non-symmetric dimer. Notably, non-symmetric dimers were the first materials for which intercalated smectic phases were observed [15–18]. A wide range of chiral dimers, both symmetric and non-symmetric, have been reported in the literature [2–4] and a central issue for study has been to determine how the form chirality of the chiral phase depends on the number of methylene groups in the flexible alkyl spacer. Cholesterol has been widely used as the chiral liquid crystal group in oligomers and polymers; for recent examples, see [19–23]. Indeed, the majority of non-symmetric chiral dimers contain a cholesteryl-based group (for recent examples, see [24–27]), and these have been the focus of considerable research interest [28] because, at least in part, they have been found to be a rich source of unusual frustrated smectic phases [29]. In this paper we report the transitional properties of a range of new non-symmetric liquid crystal dimers containing a cholesteryl-based unit, which have been designed in order to gain a better understanding of the factors controlling smectic phase formation in this class of material. The structures of these dimers together with the acronyms used to refer to them are shown in Figure 1. These particular non-symmetric dimers have been chosen for a

*Corresponding author. Email: c.t.imrie@abdn.ac.uk

ISSN 0267-8292 print/ISSN 1366-5855 online

DOI: 10.1080/02678292.2010.494412
http://www.informaworld.com

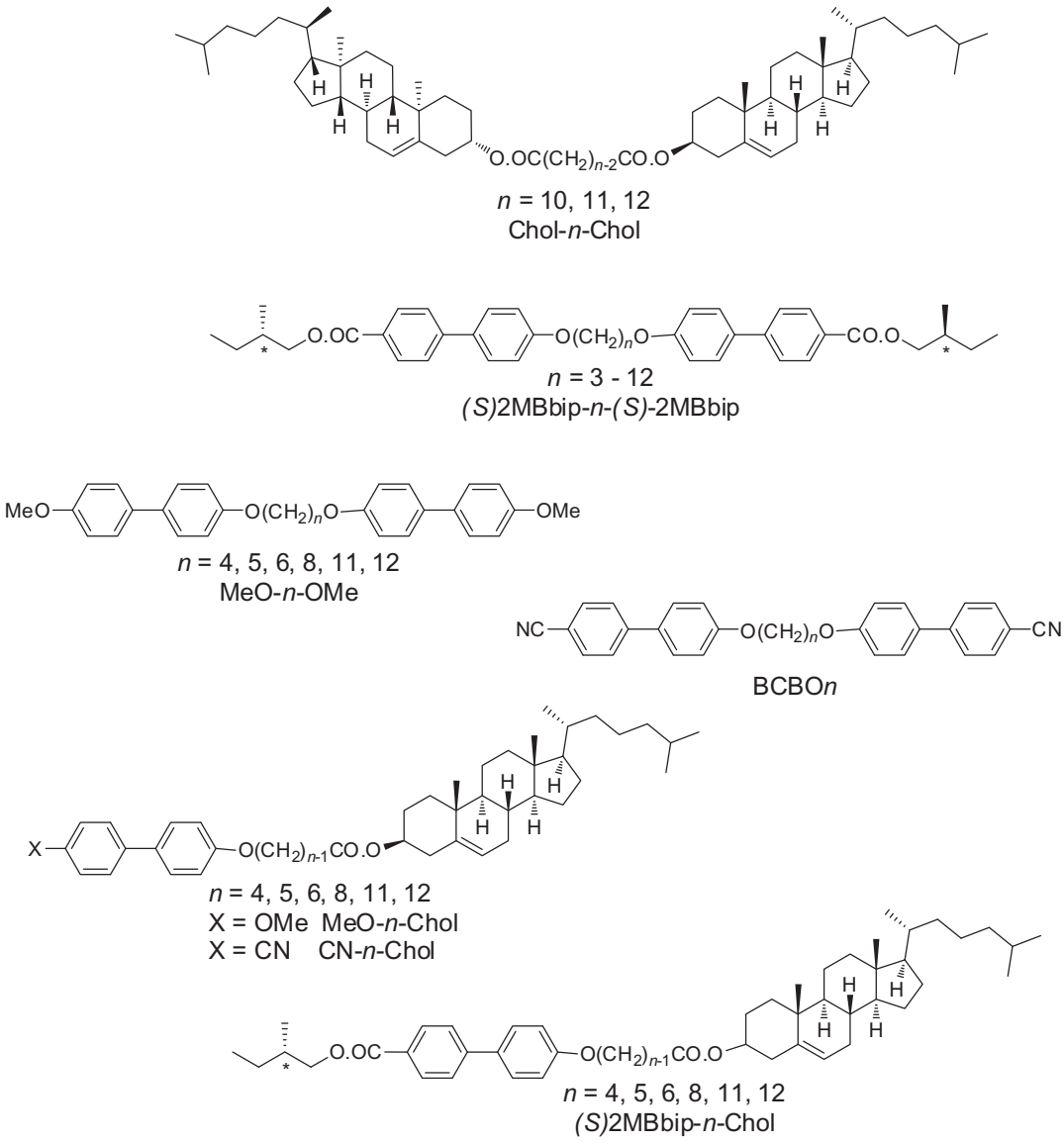

Figure 1. The structures of the symmetric and non-symmetric liquid crystal dimers together with the acronyms used to refer to them. Also shown is the structure of the α,ω-bis(4-cyanobiphenyl-4'-yloxy)alkanes, BCBO*n* [45].

number of reasons. It is widely believed that the driving force for the formation of intercalated phases by non-symmetric dimers is, at least in part, a specific interaction between the unlike mesogenic units suggested to be an electrostatic quadrupolar interaction between groups having quadrupole moments of opposite signs [30]. It is recognised, however, that steric issues also play an important role in stabilising the phase [2–4]. Thus, here we have chosen three liquid crystal groups with quite different electronic properties and steric requirements. 4-Cyanobiphenyl and 4-methoxybiphenyl have contrasting electronic properties while the 2-methyl butyl terminal chain will allow us to probe space filling constraints on the formation of smectic phases. The corresponding symmetric dimers have also been characterised to allow their behaviour to be compared with that of the non-symmetric dimers. We should note that the behaviour of some members of the Chol-*n*-Chol [31, 32] and CN-*n*-Chol [33–36] series have been reported previously.

2. Experimental

The syntheses of each series of dimers and their intermediates are described in the following sections along with representative structural characterisation data

for one member of each series. All chemicals were used as received unless stated otherwise.

2.1 Synthesis of the Chol-n-Chol series

A mixture of the appropriate α,ω-alkanedioic acid (0.5 mmol), cholesterol (1.5 mmol), N-N′-dicyclohexyl carbodiimide (DCC) (2 equiv.) and a catalytic amount of 4-dimethylaminopyridine (DMAP) in dry dichloromethane was stirred overnight at room temperature. The reaction mixture was filtered to remove the insoluble DCC complex, the filtrate collected and the solvent removed under reduced pressure. The resulting mixture was purified by column chromatography (silica) using dichloromethane as eluent. The crude product was recrystallised twice from a mixture of chloroform and ethanol. Yield = 70–80%.

2.1.1 Chol-12-Chol

^{1}H nuclear magnetic resonance (NMR) ($CDCl_3$) δ(ppm): 5.3 (t, 2H, C=C$\underline{H}$), 4.6(m, 2H, O-cholesteryl C$\underline{H}$), 2.3 (d, 4H, cholesteryl C$\underline{H}_2$, J = 8.2 Hz), 2.25 (t, 4H, $CH_2C\underline{H}_2COO$, J = 7.4 Hz), 1.95–2.23, (tt, 4H, cholestryl-$\underline{H}$), 1.8–1.9 (m, 6 H, $CH_2C\underline{H}_2CH_2COO$ and cholesteryl-$\underline{H}$), 1.4–1.6 (m, 18H, alkyl C$\underline{H}_2$ and cholesteryl-H), 1.2–1.35 (m, 22H, C$\underline{H}_2$ in alkyl spacer and terminal cholesteryl chain), 1.13–1.21 (m, 12H, cholesteryl-$\underline{H}$), 1.1 (s, 6H, CC$\underline{H}_3$), 0.9–1.3 (m, 6H, cholesteryl-$\underline{H}$), 0.92 (d, 6H, CHC$\underline{H}_3$, J = 6.7 Hz), 0.86 (dd, 12H, CH(C$\underline{H}_3$)$_2$, J = 5.0, 1.6 Hz), 0.68 (s, 6H, CC$\underline{H}_3$).

IR (KBr)ν (cm^{-1}): 2921, 2841 (CH_3, CH_2 and CH), 2211, 2178, 2031, 2015, 2000, 1970 (alkyl), 1728 (C=O), 1461, 1370 (alkyl), 1250 (C-O-C), 1164, 1084, 1026 (C–O), 1009, 955 (CH=CH), 625, 598, 569 (alkyl).

Calc. C 81.82, H 11.37%, Obs. C 81.70, H 11.52%.

2.2 Synthesis of the MeO-n-OMe series

The MeO-*n*-OMe series was prepared by the reaction of 4-hydroxy-4'-methoxybiphenyl with the appropriate α,ω-dibromoalkane. 4-Hydroxy-4'-methoxybiphenyl was prepared by the method described in detail by Craig and Imrie [36]. Thus, for MeO-11-OMe a mixture of 4-hydroxy-4'-methoxybiphenyl (2.50 mmol, 0.50 g), anhydrous potassium carbonate (4.78 mmol, 0.66 g) and 1,11-dibromoundecane (1.27 mmol, 0.40 g) in dry dimethyl foramide (DMF) (20 mL) was refluxed with stirring overnight. Water (40 mL) was added and the mixture was allowed to cool to room temperature with stirring. The precipitate was filtered, dissolved in a large amount of chloroform and filtered. Ethanol was added to the filtrate and the precipitate collected and dried under vacuum (yield 0.37 g 59%). Due to the insolubility of the MeO-*n*-OMe series in appropriate organic solvents, NMR data were not obtained. The infrared (IR) spectrum did not contain a peak corresponding to the hydroxyl group of the 4-hydroxy-4'-methoxybiphenyl starting material for which the IR spectrum had a broad peak centred around 3399 cm^{-1}. In addition, there was no apparent peak in the spectrum of the final product corresponding to the CH_2–Br stretch.

IR (KBr) n (cm^{-1}): 3015 (aromatic), 2872, 2939, 2953 (CH_2 and CH_3 str.), 1606 and 1501 (aromatic), 1039 (C–O str.), 825(Ar).

Calc. C 80.40, H 8.02%, Obs. C 80.15, H 8.04%.

2.3 Synthesis of the MeO-n-Chol series

The MeO-*n*-Chol series was prepared in two steps: first, the esterification of the appropriate ω-bromoalkanoic acid using cholesterol to give the α-bromo-(cholesteryloxycarbonyl)alkane, and the subsequent reaction of this with 4-hydroxy-4'-methoxybiphenyl to yield the MeO-*n*-Chol dimer.

2.3.1 Synthesis of 1-bromo-(cholesteryloxycarbonyl) octane

8-bromooctanoicacid (3.7 g, 16.6 mmol) was added to a mixture of cholesterol (8.4 g, 21.7 mmol), DCC (4.8 g, 23.3 mmol) and a trace of DMAP, using dichloromethane (DCM) as solvent. The mixture was allowed to stir overnight and filtered to remove any insoluble DCC complex. The filtrate was collected and the solvent removed under reduced pressure. The resulting mixture was purified by column chromatography using DCM as eluent. The crude product was recrystallised from ethanol (yield 4.5 g, 45.4%; melting point (m.p.) 87°C).

^{1}H NMR ($CDCl_3$) δ(ppm): 5.4 (d, 1H, C=C$\underline{H}$), 4.6 (m, 1H, O–C$\underline{H}$), 3.4 (t, 2H, Br–C$\underline{H}_2$–CH_2, J = 6.7 Hz), 2.4–2.2 (m, 4H, C=C–C$\underline{H}_2$–CH–O, CO_2–C$\underline{H}_2$), 2.1–0.6 (m, 51H, Br–CH_2–C$\underline{H}_2$, CO_2–CH_2–C$\underline{H}_2$, cholesteryl-C$\underline{H}$,C$\underline{H}_2$ and C$\underline{H}_3$). IR (KBr) ν (cm^{-1}): 2948, 2937, 2927, 2901, 2886, 2867, 2853 (C–H, alkyl), 1734 (C=O), 1465 (C=C), 1178 (C–O–C).

2.3.2 Synthesis of the MeO-n-Chol series

The MeO-*n*-Chol series was synthesised as described for the *(S)*MB-*n*-Chol series but using 4-hydroxy-4'-methoxybiphenyl, and the crude product was recrystallised twice from a mixture of chloroform and ethanol.

2.3.2.1 MeO-11-Chol ^{1}H NMR ($CDCl_3$) δ(ppm): 7.5–6.9 (m, 8H, Ar–H), 5.3 (t, 1H, C=C$\underline{H}$), 4.6 (m, 1H, O–C$\underline{H}$–$(CH_2)_2$), 4.0 (t, 2H,

O–C$\underline{H}_2$), 3.8 (t, 3H, OC$\underline{H}_3$), 2.4–2.2 (m, 4H, O–CH–C$\underline{H}_2$–C=CH, O–C(O)–C$\underline{H}_2$), 2.1–0.7 (m, 54H, CO_2–CH_2–C$\underline{H}$($C\underline{H}_3$)–C$\underline{H}_2$–C$\underline{H}_3$, O–CH_2–C$\underline{H}_2$ –C$\underline{H}_2$–C$\underline{H}_2$, cholesteryl-C$\underline{H}$,C$\underline{H}_2$ and C$\underline{H}_3$).

IR (KBr)ν (cm^{-1}): 2838, 2920 (alkyl), 1723 (C = O), 1602, 1495, 1462 (Ar), 1240, 1169, 1037, 1008, 817 (*p*-substitutes Ar).

Calc. C 81.17, H 10.01%, Obs. C 80.66, H 10.26%.

2.4 Synthesis of the CN-n-Chol series

The CN-*n*-Chol series was synthesised as described for the *(S)*MB-*n*-Chol series but using 4-hydroxy-4'-cyanobiphenyl and the crude product was recrystallised twice from a mixture of chloroform and ethanol.

2.4.1 CN-11-Chol

^{1}H NMR ($CDCl_3$) δ(ppm): 7.55–7.65 (quartet, 4H, NC–Ar–H), 7.4–7.5 (quartet, 2H, Ar–H), 6.9–6.95 (d, 2H, Ar–H, J = 8.6 Hz), 5.3 (t, 1H, C=CH), 4.5–4.6 (m, 1H, O-cholesteryl CH), 3.9–4.0 (t, 2H, OCH_2CH_2, J = 6.7 Hz), 2.25 (d, 2H, cholesteryl CH_2, J = 8.6 Hz), 2.2 (t, 2H, CH_2CH_2COO, J = 7.5 Hz), 1.85–1.95 (tt, 2H, cholestryl-H), 1.7–1.8 (m, 5 H, $OCH_2CH_2CH_2$ and cholesteryl-H), 1.35–1.55 (m, 12H, alkyl CH_2), 1.2–1.35 (m, 14H, CH_2 in alkyl spacer and terminal cholesteryl chain), 1.0–1.15 (m, 6H, cholesteryl-H), 0.95 (s, 3H, CCH_3), 0.85–1.0 (m, 3H, cholesteryl-H), 0.85 (d, 3H, $CHCH_3$, J = 6.7 Hz), 0.8 (dd, 6H, $CH(CH_3)_2$, J = 4.7, 2.0 Hz), 0.6 (s, 3H, $CHCH_3$).

IR (KBr)ν (cm^{-1}): 2940, 2857, 2920 (alkyl), 2218 (–CN), 1730 (C=O), 1462, 1489, 1596 (alkyl), 1251, 1170, 817 (*p*-substituted Ar), 529 (CN).

Calc. C 81.73, H 9.66, N 1.95%, Obs. C 81.51, H 9.94, N 1.75%.

2.5 Synthesis of the (S)2MBbip-n-(S)2MBbip series

The (*S*)2MBbip-*n*-(*S*)2MBbip series was prepared in two steps: first, the esterification of 4′-hydroxybiphenyl-4-carboxylic acid with (*S*)-(-)-2-methyl-1-butanol to give (*S*)-2-methyl-1-butyl-4- (4-hydroxyphenyl) benzoate, and the subsequent reaction of this with an appropriate α,ω-dibromoalkane to yield the target dimer.

2.5.1 Synthesis of (S)-2-methyl-1-butyl-4-(4-hydroxyphenyl) benzoate

(*S*)-2-methyl-1-butyl-4-(4-hydroxyphenyl) benzoate was prepared according to the method described by Ikeda *et al.* [37]. Thus, a stirred mixture of 4'-hydroxybiphenyl-4-carboxylic acid (10 g, 46.6 mmol), and (*S*)-(-)-2-methyl-1-butanol (4.93 g, 55.9 mmol), in anhydrous *n*-dibutyl ether with a small amount of sulphuric acid, was heated under reflux for three days using a Dean–Stark trap to remove the water produced. The mixture was cooled and poured into an excess of water. The resulting precipitate was extracted using diethyl ether. The ether layer was washed with aqueous sodium bicarbonate and water successively, and dried over magnesium sulphate. The ether was removed under vacuum and the crude product was recrystallised from a 1:1 mixture of toluene and hexane (yield 4.9 g, 37.1%; m.p. 114°C).

^{1}H NMR ($CDCl_3$) δ(ppm): 0.94 (3H, t, J = 7.5 Hz, CH_3), 1.03 (3H, d, J = 6.8 Hz, CH_3), 1.30 (1H, m, $ArCOOCH_2CHCH_2$), 1.51 (1H, m, $ArCOOCH_2$ $CHCH_2$), 1.85 (m, 1H, $ArCOOCH_2CH$), 4.21 (2H, m, $ArCOOCH_2$), 6.94 (2H, d, J = 8.5 Hz, ArH, 2', 6' positions), 7.61 (2h, d, J = 8.5 Hz, ArH, 2, 6, positions), 8.08 (2H, d, J = 8.5 Hz, ArH, 3, 5 positions). IR (KBr) ν (cm^{-1}): 3395 (OH str.), 2872, 2933, 2961 (CH_2 and CH_3 str.), 2887 (CH str.), 1682 (ester carbonyl str.), 1598 and 1495 (aromatic), 1285 (OH bend), 1183 and 1122 (C–O str.), 830 (*p*-disubstituted benzene).

2.5.2 Synthesis of (S)2MBbip-12-(S)2MBbip

A stirred mixture of 1,12-dibromododecane (0.35 g, 1.07 mmol), *(S)*-2-methyl-1-butyl-4- (4-hydroxyphenyl) benzoate (0.66 g, 2.32 mmol), potassium carbonate (0.59 g, 4.27 mmol) and acetone was heated at reflux for 72 h. The reaction mixture was cooled, filtered and purified by column chromatography, firstly using petroleum ether (40–60°) as an eluent to remove any unreacted dibromoalkane, and subsequently using dichloromethane as an eluent. The crude product was recrystallised from ethyl acetate (yield 0.48 g, 62.2%).

^{1}H NMR ($CDCl_3$) δ(ppm): 8.00–8.15 (4H, d, J = 8.5 Hz, ArH, 3 and 5 positions), 7.47–7.69 (8H, dd, J = 12 Hz, ArH, 2' and 6' and 2 and 6 positions), 6.90–7.05 (4H, d, J = 8.5 Hz, ArH, 3' and 5' positions), 4.07–4.28 (4H, m, $ArCOOCH_2$), 3.91–4.06 (4H, t, J = 6.7 Hz, $ArOCH_2$), 1.69–2.02 (6H, m, CH_2), 1.67–1.98 (6H, m, CH_2), 1.16–1.65 (20H, m, CH_2), 0.83–1.12 (12H, m, CH_3).

IR (KBr) ν (cm^{-1}): 2960 and 2930 cm^{-1} (CH_2 and CH_3 str.), 2861 (CH str.), 1709 (ester carbonyl str.), 1599 and 1493 (aromatic), 1189 and 1109 (C–O str.), 832 (*p*-disubstituted aromatic).

Calc. C 78.44, H 8.50%, Obs. C 78.51, H 8.65%.

2.6 Synthesis of the (S)2MBbip-n-Chol series

The (*S*)2MBbip-*n*-Chol series was prepared by the reaction of the appropriate α-bromo-(cholesteryloxycarbonyl)alkane (see Section 2.3.1) and (*S*)-2-methyl-1-butyl-4- (4-hydroxyphenyl) benzoate (see Section 2.5.1). Thus, for (*S*)2MBbip-5-Chol, a stirred mixture of 1-bromo-(cholesteryloxycarbonyl)hexane (0.27 g, 0.48 mmol),

(S)-2-methyl-1-butyl-4- (4-hydroxyphenyl) benzoate (0.16 g, 0.55 mmol) and potassium carbonate (0.29 g, 2.09 mmol) in acetone was heated under reflux for 3 days. The reaction was allowed to cool and after a short time the crude product crystallised from the mixture. The solid was collected, dissolved in dichloromethane, filtered and washed with water to remove any remaining potassium carbonate. The organic layer was dried over anhydrous magnesium sulphate. The solvent was removed under reduced pressure and the crude product recrystallised from ethanol (yield 0.13 g, 35.7%).

^{1}H NMR ($CDCl_3$) δ (ppm): 8.1 (d, 2H, Ar–H, $J = 8.2$ Hz), 7.6 (d, 2H, Ar–H, $J = 8.2$ Hz), 7.5 (d, 2H, Ar–H, $J = 8.9$ Hz), 7.0 (d, 2H, Ar–H, $J = 8.9$ Hz), 5.4 (d, 1H, C=C–H), 4.6 (m, 1H, O–CH–$(CH_2)_2$), 4.2 (m, 2H, Ar–CO_2–CH_2), 4.0 (t, 2H, O–CH_2), 2.4–2.2 (m, 4H, O–CH–CH_2–C=CH, O–C(O)–CH_2), 2.1–0.7 (m, 56H, CO_2–CH_2–CH(CH_3)–CH_2–CH_3, O–CH_2–CH_2–CH_2– CH_2, cholesteryl–CH, CH_2 and CH_3).

IR (KBr) ν (cm^{-1}): 2955, 2929, 2866, 2852 (C–H, alkyl), 1723, 1712 (C=O), 1602, 1497 (aromatic), 1469 (C=C), 1195, 1168, 1118 (C–O–C).

Elemental analysis: Calc. C, 79.85, H, 9.72%. Obs. C, 79.84, H, 9.71%.

2.7 Characterisation

The structures of the all the dimers and their intermediates were confirmed by ^{1}H NMR spectroscopy, using a Bruker AC-F 250 MHz spectrometer, and Fourier transform infrared (FTIR) spectroscopy, using an ATI Mattson Genesis Series FTIR Spectrometer. The purities of the final products were verified using elemental analysis performed by Butterworth Laboratories. The thermal behaviour of the dimers was investigated by differential scanning calorimetry (DSC) using a Mettler Toledo DSC822^e differential scanning calorimeter equipped with a TSO 801RO sample robot and calibrated using indium and zinc standards. The heating profile in all cases was heat, cool and reheat at 10° min^{-1} with a 3-min isotherm between heating and cooling segments. All samples were heated from 25°C to approximately 10° above their clearing temperatures. Thermal data were normally extracted from the second heating trace. Phase characterisation was performed using polarising light microscopy using an Olympus BH2 polarising light microscope equipped with a Linkam TMS 92 hot stage.

3. Results and discussion

3.1 Chol-n-Chol series

The transitional properties of Chol-10-Chol, Chol-11-Chol and Chol-12-Chol are listed in Table 1. For comparative purposes, Table 1 also includes the corresponding data of other members of the Chol-*n*-Chol series which have been extracted from the literature [31]. The transition temperatures of Chol-10-Chol have been reported previously [31, 32] and the data are in excellent agreement with those reported here. All three homologues synthesised as part of this study melted directly into the isotropic phase but on cooling exhibited a chiral nematic phase. This was assigned on the basis of the observation of characteristic optical textures when viewed through a polarised light microscope. Specifically, the chiral nematic phases exhibited either a fan or oily streak texture; representative textures are shown in Figure 2. The fan texture gave the characteristic Grandjean texture upon shearing. In addition, the values of the entropy change associated with the chiral nematic–isotropic transition, $\Delta S_{N^*I}/R$, are consistent with this assignment although rather low for liquid crystal dimers [2–4] and we will return to this observation later. The Chol-*n*-Chol series does not exhibit either blue or smectic phases. Both the melting, $T_{Cr\text{-}}$, and chiral nematic–isotropic transition temperatures, T_{N^*I}, decrease on increasing the spacer length for the even members of the series, which is archetypal behaviour for nematic dimers having high clearing temperatures. Chol-5-Chol does not exhibit liquid crystallinity [31] indicating that the clearing temperatures of the adjacent even-membered homologues are significantly higher such that T_{N^*I} must exhibit a pronounced alternation as the length and parity of the spacer is varied in which the even-membered dimers show the higher values. It is clear that the magnitude of this alternation decreases as the spacer length increases; for example, the isotropic phase of Chol-5-Chol can be cooled to 160°C prior to crystallisation indicating that the difference in T_{N^*I} between Chol-5-Chol and Chol-4-Chol is at least 84°C while that between Chol-11-Chol and Chol-10-Chol is 22°C. This pronounced alternation in T_{N^*I} which attenuates on increasing the spacer length is characteristic behaviour for liquid crystal dimers and has been discussed in detail elsewhere [2–4]. Such an alternation is often

Table 1. Transitional properties of the Chol-*n*-Chol series. Data for $n = 4$, 5, 6 and 8 are extracted from [31]. Brackets indicate monotropic transitions; Cr crystal, N* chiral nematic, I isotropic.

n	$T_{Cr\text{-}}$ / °C	T_{N^*I} / °C	$\Delta S_{Cr\text{-}}/R$	$\Delta S_{N^*I}/R$
4	221	244		0.99
5	198			
6	192	224		0.90
8	186	198		0.91
10	182	(179)	12.4	0.71
11	167	(157)	12.5	0.28
12	170	(168)	11.6	0.85

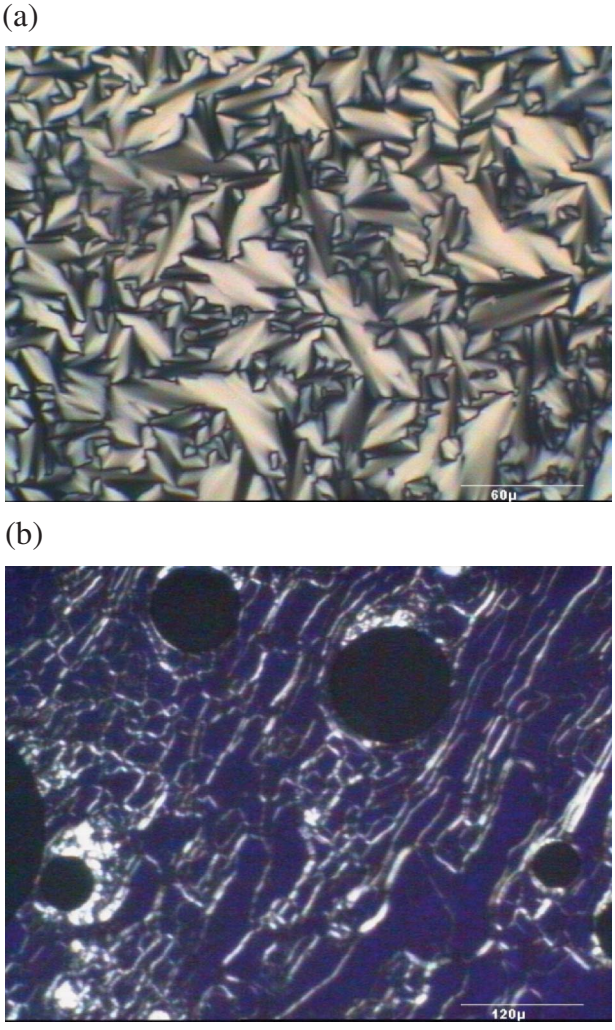

Figure 2. (a) The focal conic fan texture of the chiral nematic phase exhibited by Chol-12-Chol ($T = 167^{\circ}C$). (b) The oily streak texture of the chiral nematic phase exhibited by Chol-10-Chol ($T = 177^{\circ}C$) (colour version online).

also seen for the melting temperatures of nematic dimers as the length and parity of the spacer is varied [2–4] but this is not the case for the Chol-*n*-Chol series for which the melting point of Chol-5-Chol is higher than that of Chol-6-Chol. Given that the T_{N^*I} for Chol-5-Chol would be expected to be considerably lower than that of Chol-6-Chol, the unexpectedly high T_{CrI} of Chol-5-Chol is the reason why no liquid crystalline behaviour is observed as the mesophase would be strongly monotropic in nature. The clearing entropies, $\Delta S_{N^*I}/R$, seen for the even members of the series are considerably larger than those exhibited by Chol-11-Chol. Again this is archetypal behaviour for a series of liquid crystal dimers [2–4]. As we have noted already, however, the values of $\Delta S_{N^*I}/R$ shown by these dimers are lower than those normally observed for liquid crystal dimers containing small terminal substituents or terminal linear alkyl chains [39–43]. This may be accounted for in terms of the increased biaxiality of the cholesteryl-based unit compared to conventional rod-like mesogenic units such as, for example, cyanobiphenyl. Reduced values of $\Delta S_{NI}/R$ have also been observed for other dimers containing branched terminal chains [44, 45] or dimers in which the biaxiality of the mesogenic groups has been increased [46–48].

3.2 *(S)*2MBbip-*n*-*(S)*2MBbip series

The transitional properties of the *(S)*2MBbip-*n*-*(S)*2MBbip series are listed in Table 2. The odd members of this series did not exhibit liquid crystalline behaviour even though their isotropic phases could be extensively supercooled, typically by about 20°C, prior to crystallisation. By contrast, the even members all exhibit a chiral nematic phase although this is monotropic in nature for all but the butyl homologue. The chiral nematic phase was assigned on the basis of the observation of characteristic Grandjean planar textures, obtained on shearing fan-like textures, when viewed through the polarised light microscope. The values of $\Delta S_{N^*I}/R$ listed in Table 2 are consistent with this assignment and increase as the spacer length increases. The melting points initially show an odd–even effect as the spacer length is increased but this is quickly attenuated. T_{N^*I} decreases on increasing the spacer length for the even members of the series and by implication must exhibit a pronounced alternation across the series as the parity of the spacer is varied. As we noted in the previous section, this is characteristic behaviour for liquid crystal dimers [2–4]. It is interesting to note that blue phases were not observed on cooling the isotropic phase and prior to the formation of the chiral nematic phase for the even members

Table 2. Transition temperatures and associated entropy changes for the *(S)*2MBbip-*n*-*(S)*2MBbip series. Brackets indicate monotropic transitions; Cr crystal, N* chiral nematic, I isotropic.

n	T_{Cr-} / °C	T_{N^*I} / °C	$\Delta S_{Cr-}/R$	$\Delta S_{N^*I}/R$
3	107		11.8	
4	141	152	11.8	0.49
5	118		15.8	
6	134	(132)	14.9	0.72
7	115		15.7	
8	116	(115)	13.9	0.93
9	112		18.8	
10	118	(105)	17.9	1.09
11	111		18.9	
12	112	(102)	19.9	- [a]

Notes: [a]Crystallisation on the timescale of the DSC experiment prevented the measurement of the enthalpy change.

and we will return to this observation later. The values of $\Delta S_{N^*I}/R$ shown by these dimers are considerably lower than normally seen for liquid crystal dimers and similar observations have been made for other liquid crystal dimers containing branched terminal chains [44, 45]. As described in the previous section, this reduction in the clearing entropy has been interpreted in terms of the increased molecular biaxiality arising from chain branching [45].

3.3 MeO-n-OMe series

The transition temperatures of the MeO-*n*-OMe series are listed in Table 3. All six homologues melted directly to the isotropic phase. On cooling, however, a Schlieren texture characteristic of a nematic phase was observed in isolated droplets of each homologue when viewed through the polarised light microscope. Thus, every member of this series is assigned as a monotropic nematogen. The entropy change associated with the nematic–isotropic transition could not be determined because, on cooling, crystallisation occurred prior to the formation of the nematic phase in the DSC experiments. Both the T_m and T_{NI} of an even-membered homologue are higher than those of an adjacent odd member of the series and this difference decreases as the spacer length increases. Again, this is characteristic behaviour within a homologous series of liquid crystal dimers [2–4].

For comparative purposes, Table 3 also lists the transition temperatures of the corresponding members of the BCBO*n* series [43] in which the methoxy terminal group has been replaced by a nitrile group; see Figure 1. In contrast to the monotropic nematic behaviour seen for the MeO-*n*-OMe series, all the corresponding members of the BCBO*n* series exhibit enantiotropic nematic behcaviour. Terminal methoxy and nitrile substituents are often observed to be rather similar in their ability to promote nematic behaviour both in conventional low molar mass mesogens as well as in liquid crystal dimers [49]. Indeed, comparing the T_{NI} for the MeO-*n*-OMe and BCBO*n* series, those of the BCBO*n* series are on average just 14°C higher. By contrast, the melting temperatures of the MeO-*n*-OMe series are on average some 57°C higher than those of the BCBO*n* series and it is these much higher melting points which account for the monotropic nature of the MeO-*n*-OMe series. These higher melting points suggest that the MeO-*n*-OMe dimers can pack more efficiently into the crystal lattice.

Table 3. Transition temperatures of the MeO-*n*-OMe series. Also listed are the transition temperatures of the corresponding members of the BCBO*n* series [45]. Brackets indicate monotropic transitions; Cr crystal, N nematic, I isotropic.

	MeO-*n*-OMe			BCBO*n*		
n	T_{CrI} / °C	$\Delta S_{Cr}/R$	T_{NI} / °C	T_{CrN} / °C	T_{NI} / °C	$\Delta S_{NI}/R$
4	261	15.8	(238)	209	250	1.77
5	216	16.9	(162)	137	186	0.54
6	237	17.3	(212)	187	221	1.95
8	223	7.02	(183)	175	201	1.98
11	182	17.2	(151)	123	164	0.94
12	205	23.3	(161)	152	169	2.14

3.4 MeO-n-Chol series

The transitional properties of the MeO-*n*-Chol series are listed in Table 4. All six members exhibit an enantiotropic chiral nematic phase that was assigned on the basis of the observation of either an oily streak texture or a fan texture which sheared to give the characteristic Grandjean texture. In addition, on slow cooling the isotropic phase of MeO-5-Chol and MeO-11-Chol, a narrow temperature range blue phase was observed. The T_{N^*I} of the two odd members are lower than those of the adjacent even members with the difference being larger for the members having the shorter spacers. This implies a pronounced alternation in T_{N^*I} which attenuates as the spacer length is increased. The measured values of $\Delta S_{N^*I}/R$ also imply that there is a large odd–even effect in $\Delta S_{N^*I}/R$ as the length and parity of the spacer is varied but which appears not to attenuate. The values of $\Delta S_{N^*I}/R$ measured for this series, although larger than those seen for the Chol-*n*-Chol series, are rather low for liquid crystal dimers. Again, this may be attributed to the increased molecular biaxiality arising from the rather bulky cholesteryl unit.

3.5 CN-n-Chol series

The transitional properties of the CN-*n*-Chol series are listed in Table 5. The thermal behaviour of a number of the members of this series has been published previously

Table 4. Transitional properties of the MeO-*n*-Chol series. Cr crystal, N* chiral nematic, I isotropic.

n	T_{CrN^*} / °C	T_{N^*I} / °C	$\Delta S_{Cr}/R$	$\Delta S_{N^*I}/R$
4	150	217	6.15	1.01
5[a]	111	159	6.66	0.42
6	126	201	7.43	1.18
8	102	181	9.14	1.40
11[a]	96	143	13.8	0.69
12	102	154	9.63	1.72

Notes: [a]Exhibits a narrow temperature blue phase on cooling the isotropic phase.

Table 5. Transitional properties of the CN-*n*-Chol series. T_g glass transition temperature, Cr crystal, N* chiral nematic, I isotropic. Brackets denote monotropic phase transitions.

n	T_g / °C	T_{Cr-} / °C	T_{SmAN*} / °C	T_{N*I} / °C	$\Delta S_{Cr}/R$	$\Delta S_{SmAN*}/R$	$\Delta S_{N*I}/R$
4		159	201	225	6.89	0.21	1.19
5[a]	25	92	144	168	5.70	0.16	0.43
6	20	127	168	204	5.93	0.16	1.23
8	19	126	137	185	9.47	0.34	1.33
11	17	92	(93)	153	9.33	0.41	0.77
12	10	102	(97)	157	9.28	0.24	1.37

Notes: [a]A narrow temperature range blue phase is observed on slow cooling the isotropic phase prior to the formation of the chiral nematic phase.

and our data are in excellent agreement with those in the literature [33, 34]. All six homologues exhibited an enantiotropic chiral nematic phase that was assigned on the basis of the observation of either an oily streak texture or a fan texture which sheared to give the characteristic Grandjean texture. On cooling the chiral nematic phase of each homologue, a focal conic fan texture developed with coexisting regions of homeotropic alignment. This was assigned as a smectic A phase. In addition, on slow cooling the isotropic phase of NC-5-Chol, a blue phase developed prior to the formation of the chiral nematic phase. Marcelis *et al.* [35] have reported that the smectic A–N* transition exhibited by the members in this series with $n = 3$–8 and 11 are all accompanied by a twist grain boundary phase and for $n = 3$, 5 and 7 a blue phase is observed on slow cooling the isotropic phase. Although the transition temperatures reported here show excellent agreement with the corresponding dimers prepared by Marcelis *et al.* [33, 34] we did not observe the twist grain boundary (TGB) phases.

On cooling the smectic A phase for each homologue, except $n = 4$, a smectic glass formed. On reheating this glass, cold crystallisation occurred prior to the melting transition. The glass transition temperatures decrease on increasing spacer length presumably implying increased plasticisation on increasing the flexibility of the spacer. This is consistent with the interpretation of the dependence of the glass transition temperatures exhibited by side-chain liquid crystal polymers on the length of the flexible spacer linking the mesogenic unit to the polymer backbone [50].

The N*–I transition temperatures and associated entropy changes for this series exhibit the pronounced odd–even effect already discussed for the other dimer series. Again the values of the entropy changes associated with the N*–I transition are rather low for liquid crystal dimers. The value of the entropy change associated with the SmA–N* transition for the undecyl member is actually greater than that exhibited by the adjacent even members and such an inversion in the sense of the alternation in the odd–even effect has been observed in other series of liquid crystal dimers although its physical significance is not clear.

The layer spacings have been measured in the smectic A phases exhibited by CN-5-Chol and CN-6-Chol to be 58 Å and 65 Å, respectively. Again these are in good agreement with data reported by Marcelis *et al.* [35]. The estimated all-*trans* molecular lengths of CN-5-Chol and CN-6-Chol are 33.2 Å and 34.7 Å, respectively, such that the ratio of layer spacing to molecular length, *d*/*l*, is approximately 1.8. This implies an interdigitated arrangement of the dimers stabilised by the electrostatic interaction between the polar and polarisable cyanobiphenyl groups while space is filled efficiently in such a structure because the cross-sectional area of the cholesteryl unit is larger than that of the biphenyl group [35]. This observation is in agreement with the more general result reported by Lee *et al.* [51] that cholesteryl-based non-symmetric dimers containing an aromatic mesogenic unit having an electron-attracting terminal group have a tendency to exhibit interdigitated smectic A phases. Recently, Zhang *et al.* [36] have reported that the smectic A phase shown by CN-4-Chol has a monolayer arrangement of the dimers with an associated *d*/*l* ratio of approximately 1. The molecular significance of this surprising result is not clear.

3.6 *(S)2MBbip-n-Chol series*

The transitional properties of the (*S*)2MBbip-*n*-Chol series are listed in Table 6 and all six members exhibit enantiotropic liquid crystal phases. On cooling the isotropic phase of (*S*)2MBbip-4-Chol, a fan-like texture develops characteristic of the chiral nematic phase (see Figure 3(a)), which on further cooling changes to a filament texture (see Figure 3(b)) typical of a homeotropically aligned twist grain boundary phase. This phase exists over a very narrow temperature range and converts into a focal conic fan texture in co-existence with regions of homeotropic alignment indicative of a smectic A phase (see Figure 3(c)). For

Table 6. Transitional properties of the *(S)*2MBbip-*n*-Chol series. Cr crystal, N* chiral nematic, I isotropic.

n	T_{Cr-}	T_{SmAN*}	T_{N*I} $^{\dagger}T_{SmAI}$	$\Delta S_{Cr-}/R$	$\Delta S_{SmAN*}/R$	$\Delta S_{N*I}/R$ $^{\dagger}\Delta S_{SmAI}/R$
4	152	178[a]	190	8.39	0.25	0.76
5	123	(108)	123	9.81	0.15	0.33
6	128	143	168	7.51	0.36	0.93
8	101	141	152	9.31	0.77	1.00
11	85	100	116	12.45	0.38	0.47
12	97		†133	11.96		†2.76

Notes: [a]A short temperature range twist grain boundary A(TGBA) phase is observed at the SmA–N* transition.

$n = 5, 6, 8$ and 11, a chiral nematic phase was observed and on cooling this transformed into a smectic A phase but no intermediate twist grain boundary phase was seen. For the dodecyl member only a smectic A phase was seen. Blue phases were not observed for this series. The entropy changes associated with the chiral nematic–isotropic transition are twice as large for even than odd members but rather low when compared to conventional liquid crystal dimers. This may be accounted for in terms of the increased molecular biaxiality associated with these dimers. Similarly, the entropy change associated with the smectic A–isotropic transition for (*S*)2MBbip-12-Chol is considerably lower than that normally measured for an even-membered liquid crystal dimer [39].

Small-angle X-ray scattering (SAXS) was used to investigate the molecular organisation within the SmA phases exhibited by the (*S*)2MBbip-*n*-Chol series and representative SAXS patterns are shown in Figure 4 while their intensity profiles are shown in Figure 5. The patterns each consist of a sharp first-order reflection and, in addition, the pattern obtained for (*S*)2MBbip-6-Chol contains a diffuse peak at lower angles. The corresponding smectic layer spacings are listed in Table 7, along with the estimated all-*trans* molecular lengths. The layer spacings for (*S*)2MBbip-4-Chol and (*S*)2MBbip-5-Chol are approximately equal to the estimated all-*trans* molecular lengths of the dimers implying that the molecules are forming a monolayer smectic A phase. By comparison, the ratio of the layer spacing to the estimated all-*trans* molecular length for the smectic A phase exhibited by (*S*)2MBbip-8-Chol, (*S*)2MBbip-11-Chol and (*S*)2MBbip-12-Chol is approximately 0.5. This suggests that these dimers are forming an intercalated smectic A phase in which the different mesogenic moieties are overlapping while the alkyl chains constitute

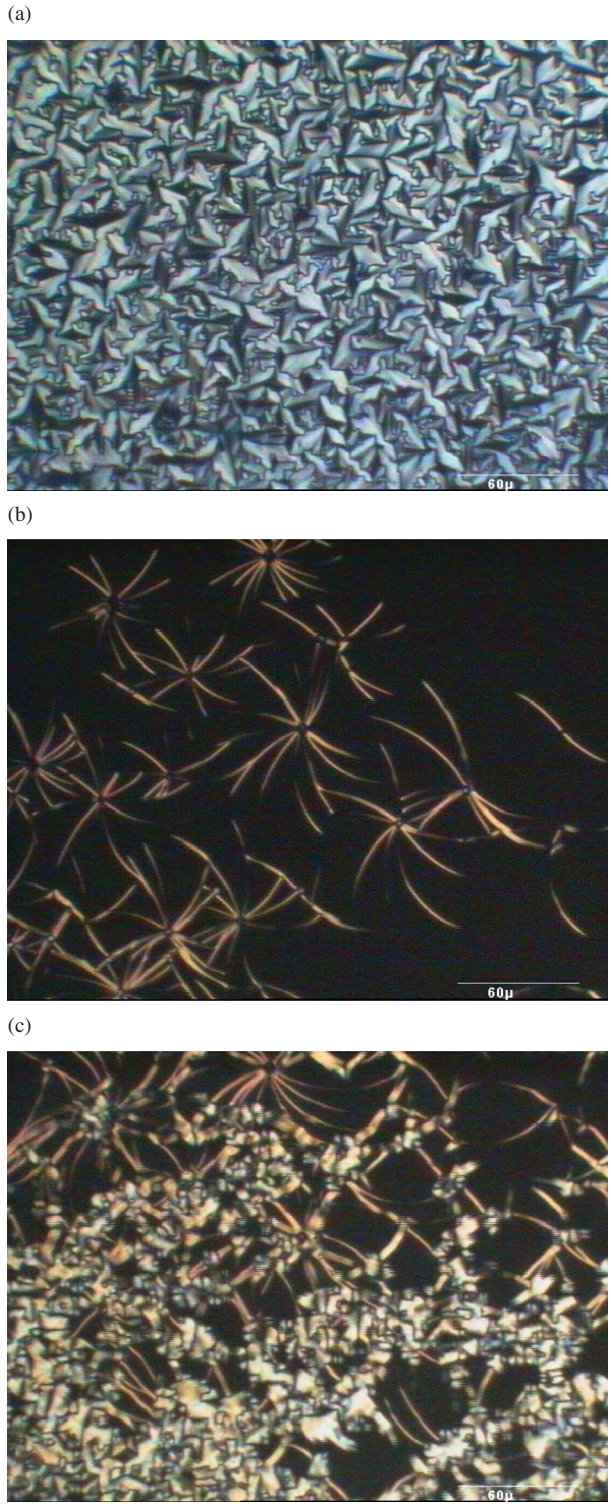

Figure 3. (a) The focal conic fan texture of the chiral nematic phase, (b) the filament texture of the TGB phase and (c) the optical texture at the TGB–SmA transition exhibited by (*S*)2MBbip-4-Chol.

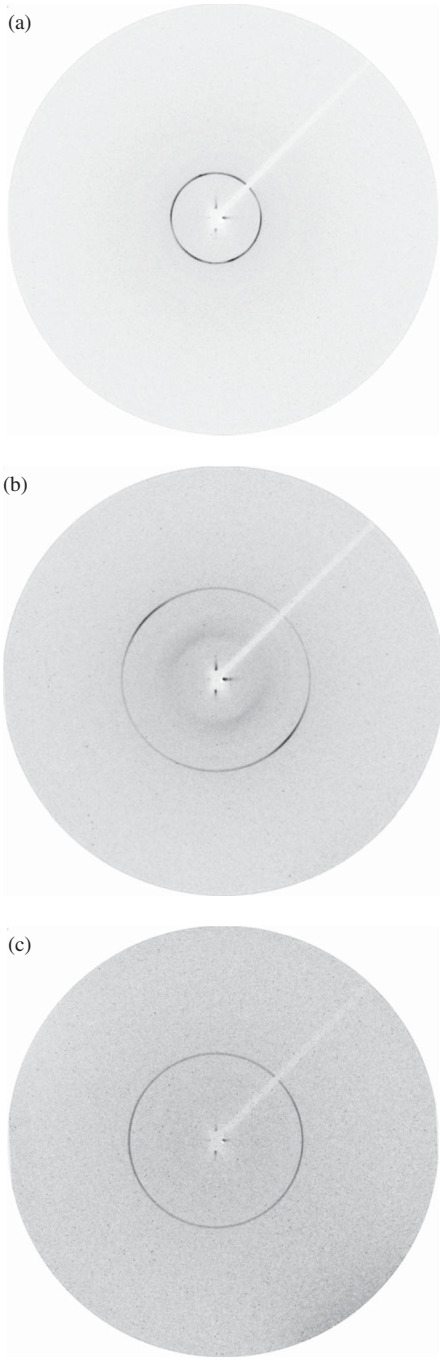

Figure 4. The X-ray patterns for the smectic A phases exhibited by (a) (*S*)2MBbip-4-Chol ($T = 160^{\circ}$C), (b) (*S*)2MBbip-6-Chol ($T = 138^{\circ}$C) and (c) (*S*)2MBbip-8-Chol ($T = 110^{\circ}$C).

another microdomain. This shift from a monolayer to an intercalated arrangement on increasing spacer length has been observed for structurally similar liquid crystal dimers containing a cholesteryl-based group [35]. The sharp first-order reflection seen in the SAXS pattern obtained for the smectic A phase exhibited by (*S*)2MBbip-6-Chol corresponds to a layer spacing of 19.7 Å implying an intercalated arrangement of the dimers. The diffuse peak observed in this SAXS pattern, however, corresponds to a periodicity of 39.7 Å which is similar to the estimated molecular length of (*S*)2MBbip-6-Chol. Thus, in the intercalated smectic A phase there exist short-range incommensurate structural fluctuations associated with the monolayer smectic A phase. To our knowledge, such incommensurate structural fluctuations have not previously been reported in materials of this specific type on increasing spacer length, although incommensurate phases have been observed for other cholesterol-based non-symmetric dimers [29, 52, 53] and hydrogen-bonded analogues [54, 55]. It is interesting to note that these incommensurate structural fluctuations were not observed for the corresponding alkoxybiphenyl-containing dimers for which, or increasing spacer length, exclusively nematic behaviour is observed for dimers of intermediate spacer length while a monolayer smectic A phase is observed for short spacer lengths and an intercalated smectic A phase for longer spacer lengths [35].

The intercalated smectic A phase is sketched in Figure 6 and may be thought of in terms of two microphase separated domains. In one of these the differing mesogenic units are mixed while the other is composed of the spacers and terminal chains. The ability to accommodate the terminal chains into this arrangement is determined largely by the length of the flexible spacer. Thus, for short spacer lengths, (*S*)2MBbip-4-Chol and (*S*)2MBbip-5-Chol, there is simply insufficient space to accommodate the terminal chains and the monolayer smectic A phase is observed. Monolayer smectic A phases have been observed for similar dimers when the terminal chain length exceeds that of the spacer [56]. For the dimers containing longer spacers, the terminal chains can be accommodated within the structure and the intercalated smectic A phase is observed. We will return to a discussion of the driving force for the formation of the intercalated smectic A phase by these dimers later.

4. Comparison of the non-symmetric dimer series

In order to compare the transition temperatures of the non-symmetric dimers, T_{AB}, with those of the corresponding parent symmetric dimers, T_A and T_B, we use a scaled deviation defined as [16]

$$\Delta T_{\mathrm{SC}} = \frac{2T_{AB} - (T_A + T_B)}{(T_A + T_B)}.$$

We should note that the nature of the clearing transitions we are comparing in some instances differ but for the majority of liquid crystal series the smectic–isotropic

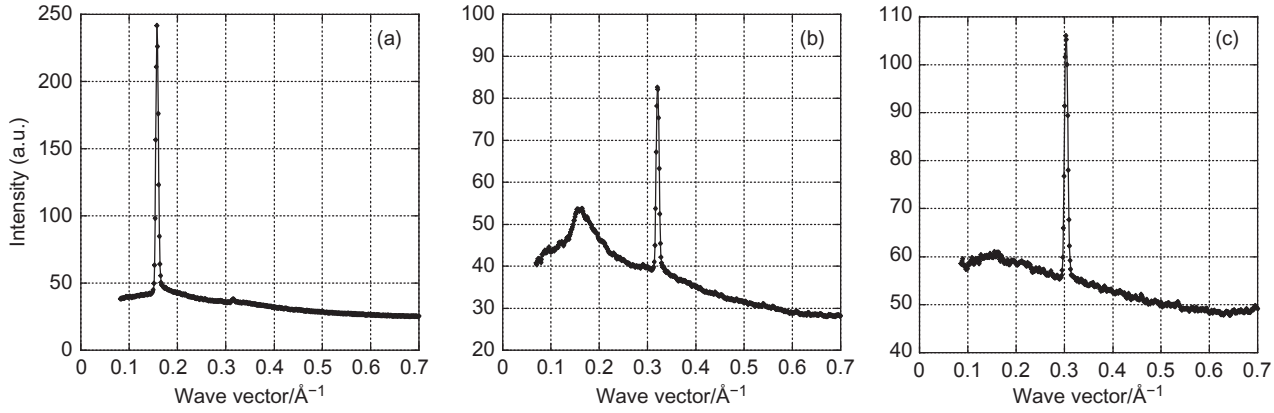

Figure 5. The intensity profiles of the X-ray patterns obtained for the smectic A phases exhibited by (a) (*S*)2MBbip-4-Chol, (b) (*S*)2MBbip-6-Chol and (c) (*S*)2MBbip-8-Chol shown in Figure 4.

Table 7. The smectic A layer spacings, *d*, measured using X-ray diffraction for the (*S*)2MBbip-*n*-Chol series, together with the estimated all *trans* molecular lengths, *l*, and the corresponding *d*/*l* ratios.

n	4	5	6	8	11	12
d/Å	40	40.5	19.7 <39.7>	20.7	21.9	22.6
l/Å	34	36.8	38.0	42.9	45.8	46.5
d/*l*	1.2	1.1	0.52	0.48	0.48	0.49

Note: < > denotes diffuse scattering, not a resolution limited peak.

transition temperatures can be obtained from an extrapolation of the nematic–isotropic transition temperatures. We believe that this observation justifies our approach.

Before we discuss the values of ΔT_{SC} for the dimers reported here, we should first consider the behaviour of an ideal binary mixture of nematogens for which $\Delta T_{SC} = 0$. The phase diagrams for binary mixtures of nematogens have been successfully predicted using a molecular field theory in which three intermolecular energy parameters, ε_{AA}, ε_{BB} and the mixed parameter, ε_{AB}, must be defined [57]. The parameters describing the interactions between like species, ε_{AA} and ε_{BB}, are proportional to the nematic–isotropic transition temperatures of the pure components. If the interaction parameter between the unlike species, ε_{AB}, is assumed to be the geometric mean of ε_{AA} and ε_{BB}, then T_{NI} of the mixture is simply the weighted average of those of the components. Thus, T_{NI} of the mixture depends linearly on composition and $\Delta T_{SC} = 0$. This behaviour is often found experimentally. If, however, ε_{AB} is allowed to deviate away from the geometric mean approximation then T_{NI} of the mixture no longer shows a linear dependence on composition but instead, if the deviation in ε_{AB} is a positive one, then T_{NI} exhibits a curve lying above the straight line

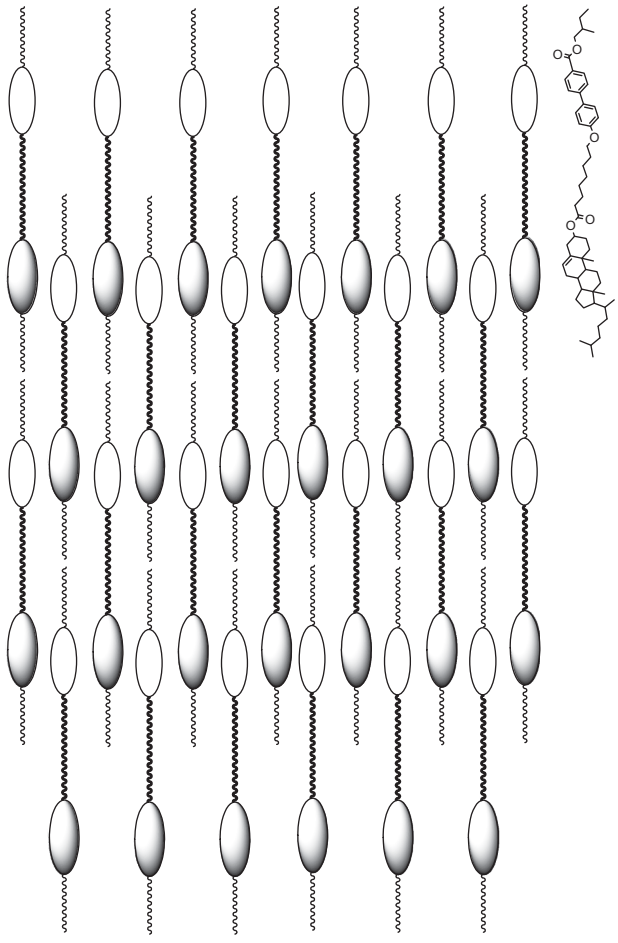

Figure 6. A sketch of the intercalated smectic A phase.

such $\Delta T_{SC} > 0$. Conversely, if the deviation in ε_{AB} is negative, then T_{NI} shows a curve lying below the straight line and $\Delta T_{SC} < 0$ [58]. Within this theoretical approach the nematogens are assumed to be rigid, cylindrically symmetric particles but ΔT_{SC} has also been calculated using the Marcelja–Luckhurst theory

Table 8. Scaled deviations in transition temperatures, ΔT_{SC}, for the non-symmetric dimers when compared to those of the parent symmetric dimers. The values of ΔT_{SC} are expressed as percentages.

	ΔT_{SC} (Melting) /%			ΔT_{SC} (Clearing) /%		
	MeO-*n*-Chol	**CN-*n*-Chol**	***(S)*2MBbip-*n*-Chol**	**MeO-*n*-Chol**	**CN-*n*-Chol**	***(S)*2MBbip-*n*-Chol**
4	–17.7	–11.5	–6.4	–4.7	–4.2	–1.7
5	–20.0	–17.1	–8.1			
6	–18.2	–13.5	–8.0	–3.5	–3.7	–2.2
8	–21.5	–12.0	–11.8	–2.1	–3.1	–1.1
11	–17.5	–12.7	–13.1	–2.6	–1.7	
12	–18.6	–13.6	–10.6	–2.4	–2.6	–0.5

of nematogens composed of flexible molecules [16]. This revealed a qualitative disagreement between the experimental values of ΔT_{SC} for a series of non-symmetric dimers and those predicted by theory which was attributed to ε_{AB} deviating from the geometric mean approximation. Thus non-zero values of ΔT_{SC} provide evidence for specific molecular interactions between the unlike groups in a non-symmetric dimer.

The calculated scaled deviations, ΔT_{SC}, in the melting and clearing temperatures are listed in Table 8. All the values of ΔT_{SC} for the melting transition are negative and, with just a single exception, for any given spacer length, ΔT_{SC} is largest for the MeO-*n*-Chol series and smallest for the (*S*)2MBbip-*n*-Chol series. It is unwise to speculate on the molecular significance of these values without a detailed knowledge of the crystal structures involved but the relative magnitudes of ΔT_{SC} may reflect the steric mismatch between the methoxybiphenyl and cholesteryl-based groups which would disrupt the crystal packing.

The values of ΔT_{SC} associated with the clearing transition are also all negative but considerably smaller than those associated with the melting transition. Within a given series, ΔT_{SC} tends to become more positive as the spacer length is increased. The values of ΔT_{SC} are similar to those observed for other series of non-symmetric dimers [16]. These deviations are difficult to interpret at a molecular level but, as noted earlier, do provide evidence for a specific interaction between the unlike mesogenic groups. We will return to this issue later.

We now turn our attention to the phase behaviour exhibited by these dimers. Blue phases are only observed for a small number and exclusively odd-membered homologues. This is in accordance with what has emerged to be a rather general observation made by Blatch *et al.* [44] that blue phases are observed for odd-membered non-symmetric dimers and not their even spacer counterparts. The authors attributed this observation to the smaller pitch found for odd-membered dimers relative to even members which arises from the smaller twist elastic constant of odd dimers related to their lower orientational order.

The four sets of parent symmetric dimers show only nematic behaviour whereas the corresponding non-symmetric dimers do exhibit smectic behaviour. In the case of the CN-*n*-Chol series, all the homologues studied exhibited an interdigitated smectic A phase which is stabilised by the electrostatic interaction between the polar and polarisable cyanobiphenyl groups. The driving force for the formation of the smectic phase may be the difference in steric bulk between the cholesteryl and cyanobiphenyl groups such that in an interdigitated phase, space is filled efficiently. It is interesting to note that the negative values of ΔT_{SC} observed for the CN-*n*-Chol series strongly suggest a specific interaction between the unlike mesogenic units but this does not drive the formation of an intercalated smectic phase. By contrast, the longer members of the (*S*)2MBbip-*n*-Chol series do exhibit an intercalated smectic A phase. The formation of smectic phases in non-symmetric dimers containing cholesteryl has been interpreted in terms of a subtle balance between the electrostatic interactions between the cholesteryl and aromatic-based units and the van der Waals interactions between the cholesteryl segment and other aliphatic chains [59, 60]. In the (*S*)2MBbip-*n*-Chol series it is possible that the specific interaction between the unlike mesogenic units involves electrostatic interactions between the electron rich carbonyl linking group attached to the cholesteryl unit and the electron deficient aromatic unit. For this interaction to be accommodated within an intercalated arrangement the length of the spacer must exceed those of the terminal chains and thus an intercalated smectic A phase is observed only for the longer homologues. For the shortest homologues there is simply insufficient space within the intercalated arrangement to accommodate the terminal chains and, hence, a monolayer smectic A phase is observed, stabilised by interactions between the aliphatic chains and the cholesteryl unit. For (*S*)2MBbip-6-Chol the competition between these two

driving forces means an intercalated smectic A phase is formed but in co-existence with strong fluctuations associated with the monolayer arrangement. The absence of smectic behaviour for the MeO-*n*-Chol series may now be understood. The biphenyl unit is electron rich so changing the nature of the electrostatic interaction while the van der Waals interactions between the cholesteryl unit and terminal chains are also reduced. Increasing the length of the alkoxy chain does promote intercalated smectic behaviour [35] highlighting the importance of the van der Waals interactions.

5. Conclusions

The smectic behaviour of the CN-*n*-Chol and (*S*)2MBbip-*n*-Chol dimers has been attributed to a subtle interplay of electrostatic and van der Waals interactions. For the CN-*n*-Chol series, interdigitated smectic A phases are observed and stabilised by the electrostatic interaction between the polar and polarisable cyanobiphenyl groups while space is filled efficiently because of the mismatch in the cross-sectional areas of the cholesteryl and biphenyl groups. By comparison, the intercalated smectic behaviour of the (*S*)2MBbip-*n*-Chol series is driven by the electrostatic interaction between the electron-rich carbonyl linking group attached to the cholesteryl unit and the electron deficient aromatic unit. These interactions cannot be accommodated in an intercalated arrangement for short spacer lengths and instead a monolayer structure is observed stabilised by van der Waals interactions between the cholesteryl-group and alkyl chains. Smectic behaviour is not observed for the MeO-*n*-Chol series as the biphenyl group is electron rich while the absence of a terminal chain has reduced the cholesteryl-alkyl chain interactions. It is interesting to note that for these non-symmetric dimers, blue phases have only been observed for certain odd-membered homologues in accordance with the rather general observation that blue phases are observed for odd-membered non-symmetric dimers and not their even-membered counterparts.

References

[1] Goodby, J.W.; Saez, I.M.; Cowling, S.J.; Gasowska, J.S.; MacDonald, R.A.; Sia, S.; Watson, P.; Toyne, K.J.; Hird, M.; Lewis, R.A.; Lee, S.E.; Vaschenko, V. *Liq. Cryst.* **2009**, *36*, 567–605.

[2] Imrie, C.T. *Struct. Bonding* **1999**, *95*, 149–192.

[3] Imrie, C.T.; Henderson, P.A. *Curr. Opin. Colloid Interface Sci.* **2002**, *7*, 298–311.

[4] Imrie, C.T.; Henderson, P.A. *Chem. Soc. Rev.* **2007**, *36*, 2096–2124.

[5] Imrie, C.T.; Henderson, P.A.; Yeap, G.Y. *Liq. Cryst.* **2009**, *36*, 755–777.

[6] Toh, C.L.; Xu, J.; Lu, X.; He, C. *Liq. Cryst*. **2008**, *35*, 241–251.

[7] Bai, B.; Wang, H.; Zhang, P.; Qu, S.; Li, F.; Yu, Z.; Long, B.; Li, M. *Liq. Cryst*. **2008**, *35*, 793–798.

[8] Wang, H.; Shao, R.; Zhu, C.; Bai, B.; Gong, C.; Zhang, P.; Li, F.; Li, M.; Clark, N.A. *Liq. Cryst*. **2008**, *35*, 967–974.

[9] Centore, R. *Liq. Cryst.* **2009**, *36*, 239–245.

[10] Bialecka-Florjanczyk, E.; Sledzinska, I.; Gorecka, E.; Przedmojski, J. *Liq. Cryst*. **2008**, *35*, 401–406.

[11] Bhowmik, P.K.; Han, H.; Nedeltchev, A.K.; Mandal, H.D.; Jimenez-Hernandez, J.A.; McGannon, P.M.; Lopez, L.; Kang, S.W.; Kumar, S. *Liq. Cryst*. **2009**, *36*, 1389–1399.

[12] Ferrarini, A.; Greco, C.; Luckhurst, G.R. *J. Mater. Chem*. **2007**, *17*, 1039–1042.

[13] Aziz, N.; Kelly, S.M.; Duffy, W.; Goulding, M. *Liq. Cryst*. **2008**, *35*, 1279–1292.

[14] Srivastava, R.M.; Filho, R.A.W.N.; Schneider, R.; Vieira, A.A.; Gallardo, H. *Liq. Cryst.* **2008**, *35*, 737–742.

[15] Hogan, J.L.; Imrie, C.T.; Luckhurst, G.R. *Liq. Cryst.* **1988**, *3*, 645–650.

[16] Attard, G.S.; Date, R.W.; Imrie, C.T.; Luckhurst, G.R.; Roskilly, S.J.; Seddon, J.M.; Taylor, L. *Liq. Cryst.* **1994**, *16*, 529–581.

[17] Imrie, C.T. *Liq. Cryst.* **2006**, *33*, 1449–1454.

[18] Attard, G.S.; Garnett, S.; Hickman, C.G.; Imrie, C.T.; Taylor, L. *Liq. Cryst.* **1990**, *7*, 495–508.

[19] Guo, J.; Sun, J.; Li, K.; Cao, H.; Yang, H. *Liq. Cryst*. **2008**, *35*, 87–97.

[20] Aldred, M.P.; Hudson, R.; Kitney, S.P.; Vlachos, P.; Liedtke, A.; Woon, K.L.; O'Neill, M.; Kelly, S.M. *Liq. Cryst.* **2008**, *35*, 413–427.

[21] Gupta, V.K.; Sharma, R.K.; Mathews, M.; Yelamaggad, C.V. *Liq. Cryst*. **2009**, *36*, 339–343.

[22] Cong, Y.H.; Wang, W.; Tian, M.; Meng, F.B.; Zhang, B.Y. *Liq. Cryst*. **2009**, *36*, 455–460.

[23] Zhan, X.; Jing, X.; Wu, C. *Liq. Cryst*. **2009**, *36*, 1349–1354.

[24] Zhang, C.; Jin, L.; Yin, B.; Jamil, M.; Jeon, Y.J. *Liq Cryst*. **2008**, *35*, 39–44.

[25] Sharma, R.K.; Gupta, V.K.; Mathews, M.; Yelamaggad, C.V. *Liq. Cryst.* **2008**, *35*, 1161–1167.

[26] Pandey, A.S.; Dhar, R.; Pandey, M.B.; Achalkumar, A.S.; Yelamaggad, C.V. *Liq. Cryst*. **2009**, *36*, 13–19.

[27] Sharma, R.K.; Gupta, V.K.; Mathews, M.; Yelamaggad, C.V. *Liq. Cryst*. **2009**, *36*, 225–230.

[28] Yelamaggad, C.V.; Shanker, G.; Hiremath, U.S.; Prasad, S.K. *J. Mater. Chem*. **2008**, *18*, 2927–2949.

[29] Hardouin, F.; Achard, M.F.; Jin, J.I.; Yun, Y.K; Chung, S.J. *Eur. Phys. J.* **1998**, *BI*, 47–56.

[30] Blatch, A.E.; Fletcher, I.D.; Luckhurst, G.R. *Liq. Cryst.* **1995**, *18*, 801–809.

[31] Marcelis, A.T.M.; Koudijs, A.; Sudhölter, E.J.R. *J. Mater. Chem.* **1996**, *6*, 1469–1472.

[32] Hanasaki, T.; Kawashima, J.; Morishita, N.; Yamamoto, T. *Mol. Cryst. Liq. Cryst.* **2001**, *365*, 15–22.

[33] Marcelis, A.T.M.; Koudijs, A.; Sudhölter, E.J.R. *Recl. Trav. Chim. Pays-Bas* **1994**, *113*, 524–526.

[34] Marcelis, A.T.M.; Koudijs, A.; Sudhölter, E.J.R. *Liq. Cryst.* **1995**, *18*, 843–850.

[35] Marcelis, A.T.M.; Koudijs, A.; Klop, E.A.; Sudhölter, E.J.R. *Liq. Cryst.* **2001**, *28*, 881–887.
[36] Zhang, H.Q.; Liu, W.K.; Zhao, L.C.; Cheng, Z.H.; Zhang, S.; Li, Y.; Yang, H. *Chinese Chem. Lett.* **2009**, *20*, 1077–1080.
[37] Craig, A.A.; Imrie, C.T. *J. Mater. Chem.* **1994**, *4*, 1705–1714.
[38] Ikeda, T.; Zushi, O.; Saski, T.; Ichimura, K.; Takezoe, H.; Fukuda, A.; Skarp, K.A.W. *Mol. Cryst. Liq. Cryst*. **1993**, *225*, 67–79.
[39] Date, R.W.; Imrie, C.T.; Luckhurst, G.R.; Seddon, J.M. *Liq. Cryst.* **1992**, *12*, 203–238.
[40] Henderson, P.A.; Niemeyer, O.; Imrie, C.T. *Liq. Cryst.* **2001**, *28*, 463–472.
[41] Henderson, P.A.; Seddon, J.M.; Imrie, C.T. *Liq. Cryst.* **2005**, *32*, 1499–1513.
[42] Henderson, P.A.; Cook, A.G.; Imrie, C.T. *Liq. Cryst.* **2004**, *31*, 1427–1434.
[43] Emsley, J.W.; Luckhurst, G.R.; Shilstone, G.N.; Sage, I. *Mol. Cryst. Liq. Cryst.* **1984**, *102*, 223–233.
[44] Blatch, A.E.; Fletcher, I.D.; Luckhurst, G.R. *J. Mater. Chem.* **1997**, *7*, 9–17.
[45] Yeap, G.Y.; Hng, T.C.; Yeap, S.Y.; Gorecka, E.; Ito, M.M.; Ueno, K.; Okamoto, M.; Mahmood, W.A.K.; Imrie, C.T. *Liq. Cryst*. **2009**, *36*, 1431–1441.
[46] Imrie, C.T. *Liq. Cryst*. **1989**, *6*, 391–396.
[47] Attard, G.S.; Imrie, C.T. *Liq. Cryst*. **1992**, *11*, 785–789.
[48] Attard, G.S.; Imrie, C.T.; Karasz, F.E. *Chem. Mater*. **1992**, *4*, 1246–1253.
[49] Gray, G.W. *The Molecular Physics of Liquid Crystals*: Luckhurst, G.R., Gray, G.W., Eds.; Academic Press, 1979; Chapter 1.
[50] Imrie, C.T.; Karasz, F.E.; Attard, G.S. *Macromolecules* **1993**, *26*, 545–550.
[51] Lee, D.W.; Jin, J.I.; Laguerre, M.; Achard, M.F.; Hardouin, F. *Liq. Cryst*. **2000**, *27*, 145–152.
[52] Hardouin, F.; Achard, M.F.; Jin, J.I.; Shin, J.W.; Yun, Y.K. *J. Physique II* **1994**, *4*, 627–643.
[53] Hardouin, F.; Achard, M.F.; Jin, J.I.; Yun, Y.K. *J. Physique II* **1995**, *5*, 927–935.
[54] Lee, J.W.; Jin, J.I.; Achard, M.F.; Hardouin, F. *Liq. Cryst.* **2001**, *28*, 663–671.
[55] Lee, J.W.; Jin, J.I.; Achard, M.F.; Hardouin, F. *Liq. Cryst.* **2003**, *30*, 1193–1199.
[56] Lee, J.W.; Park, P.; Jin, J.I.; Achard, M.F.; Hardouin, F. *J. Mater. Chem.* **2003**, *13*, 1367–1372.
[57] Humphries, R.L.; James, P.G.; Luckhurst, G.R. *Symp. Faraday Soc.* **1971**, *5*, 107–118.
[58] Humphries, R.L.; Luckhurst, G.R. *Chem. Phys. Lett.* **1973**, *23*, 567–570.
[59] Hardouin, F.; Achard, M.F.; Laguerre, M.; Jin, J.I.; Ko, D.H. *Liq. Cryst.* **1999**, *26*, 589–599.
[60] Cha, S.W.; Jin, J.I.; Laguerre, M.; Achard, M.F.; Hardouin, F. *Liq.Cryst.* **1999**, *26*, 1325–1337.